Available online at www.sciencedirect.com
ScienceDirect
Journal of Molecular Catalysis A: Chemical 270 (2007) 101–111
JOURNAL OF MOLECULAR CATALYSIS A: CHEMICAL
www.elsevier.com/locate/molcata

Pd-based sulfated zirconia prepared by a single step sol–gel procedure for lean NOx reduction

Erik M. Holmgreen, Matthew M. Yung, Umit S. Ozkan *

Department of Chemical and Biomolecular Engineering, The Ohio State University, Columbus, OH 43210, USA

Received 5 September 2006; received in revised form 13 January 2007; accepted 17 January 2007
Available online 21 January 2007

Abstract

Pd-based sulfated zirconia catalysts have been prepared through a single step (one-pot) sol–gel preparation technique, in which both sulfate and Pd precursors were dissolved in an organic solution before the gelation step. Observation of the calcination procedure through TGA/DSC and mass spectrometry revealed that the addition of increasing amounts of Pd resulted in the evolution of organic precursor species at lower temperatures. *In situ* XRD experiments showed that tetragonal zirconia is formed at lower temperatures and larger zirconia crystallites are formed when Pd is added to the gel. Although tetragonal zirconia was the only phase observed through XRD, Raman spectra of samples calcined at 700 °C showed the presence of both the tetragonal and the monoclinic phase, indicating a surface phase transition. DRIFTS experiments showed NO species adsorbed on Pd^{2+} cations. Pd/SZ catalysts prepared through this single step method were active for the reduction of NO_2 with CH_4 under lean conditions. Calcination temperature had a significant effect on this activity, with samples calcined at 700 °C being much more active than those calcined at 600 °C, despite the observed transition to the monoclinic phase. This activity may be linked to observed changes in the surface sulfate species at higher calcination temperatures.

Keywords: Palladium; Sulfated zirconia; Sol–gel; DRIFTS; Lean NOx reduction

1. Introduction

The reduction of nitrogen oxides (NOx) with methane is an attractive approach to pollution control, due to methane availability through the natural gas infrastructure. Such a technology would be particularly applicable to stationary natural gas engines, in which unburned methane remains as a component in the exhaust. To improve efficiency, however, these engines typically operate under lean conditions. This presents a challenge to the selective reduction of NOx, as hydrocarbon combustion with O_2 tends to deplete the reducing agent [1,2]. This is particularly important for Pd-based NOx reduction catalysts, as Pd can have high activity for the combustion reaction. Nishizaka and Misono [3,4] showed that Pd supported on H-ZSM-5 was selective for the reduction of NOx under lean conditions and linked this activity to the acidity of the support material. Resasco and co-workers [5,6] extended this link to acidity by demonstrating that non-zeolite acidic supports, including sulfated zirconia, also produced selective NO reduction catalysts. The selectivity of Pd-based acidic catalysts has been linked to Pd^{2+} ions, which are selective for the NOx reduction reaction. The presence of these Pd species has been confirmed through both EXAFS [7] and TPR [8] studies. Ohtsuka [9] observed higher activity for the reduction of NO_2 with CH_4 than for the reduction of NO with CH_4 over Pd/SZ catalysts, while Pt/SZ was observed to be active for the oxidation of NO to NO_2. Based on these observations, they reported preparation of an active bimetallic catalyst [10].

Common preparations of sulfated zirconia involve the treatment of precipitated zirconium hydroxide with either ammonium sulfate or sulfuric acid prior to calcination [11]. More recently, the preparation of sulfated zirconia catalysts, which are generally accepted as strong acid catalysts, through sol–gel preparation techniques has been investigated [12]. Several authors have made use of one-step methods in which incorporation of sulfur is achieved by addition prior to the gelation step [13,14]. Preparation through these sol–gel methods allows for better control of structural and textural properties, as

* Corresponding author. Tel.: +1 614 292 6623; fax: +1 614 292 3769.
E-mail address: ozkan.1@osu.edu (U.S. Ozkan).

1381-1169/$ – see front matter © 2007 Elsevier B.V. All rights reserved.
doi:10.1016/j.molcata.2007.01.030

well as sulfur content of the catalysts, through solvent selection [15] or hydrolysis method [16,17]. In a single-step sol–gel preparation, Ardizzone et al. observed the formation of different sulfate species with varying pH during catalyst preparation, which corresponded to activity differences in the conversion of benzoic acid [18]. Comparisons of *in situ* and *ex situ* sulfation procedures in Zr–Si materials have been shown to result in the formation of different Zr species on the catalyst surface [19], and that these sulfation steps occur through different mechanisms [20]. Promotion by the incorporation of metals to the single-step sol–gel preparation has been shown to modify catalyst activities. Ga was observed to increase dehydrogenation of C_6 hydrocarbons through either participating as redox sites or by increasing the number of Lewis acid sites present on the catalyst [12]. Morterra et al. incorporated Pt to a sol–gel sulfated zirconia [21]. They observed similar surface areas for different Pt and sulfate loadings, and that sulfate species became more labile with the incorporation of Pt into the catalyst. Of particular interest is that the authors observed that monoclinic sulfated zirconia prepared by their one-pot preparation retained a high level of sulfate groups and were catalytically active, in contrast to results obtained through other preparations.

We have previously studied a series of Pd/TiO_2 catalysts, active for NO reduction with CH_4, that were prepared by both incipient wetness and single step sol–gel techniques [22,23]. In these catalysts, the oxidation state of Pd was determined to be vital for activity, with metallic Pd leading to the formation of key reaction intermediates. Pd/TiO_2 prepared by a single step sol–gel technique was shown to be more resistant to deactivation through oxidation of the Pd. The stability of the active sites in these catalysts was proposed to be due to 'anchoring' of Pd species to the support through the modified sol–gel technique [24].

We have also previously reported the activity of Pd supported on monoclinic sulfated zirconia prepared by impregnation [25] in NO_2 reduction with methane. We have also demonstrated that these catalysts can be used in a dual catalyst scheme, in conjunction with an oxidation catalyst, to reduce NO with CH_4 under lean conditions [26]. In this scheme, the oxidation catalyst would convert NO to NO_2, and NO_2 would be reduced with CH_4 over the Pd/SZ catalysts. In this paper we explore a single step sol–gel technique as a method of producing active catalysts for the reduction of NO_2 with CH_4. The effects of Pd loading and calcination temperature on the catalyst structure and activity are examined.

2. Experimental

2.1. Catalyst preparation

Pd-based sulfated zirconia catalysts were prepared using a 'one-pot' sol–gel technique in which all the catalyst components were added to solution before gelation. This preparation was similar to that used by Hamouda and Ghorbel [27], making use of acetic acid as a controlled hydrolysis agent. Sol–gel catalysts were prepared using *n*-propanol as a solvent. In the Pd-containing samples, Pd acetate was first dissolved in the propanol under constant stirring. The amounts of Pd that were added produced final catalyst loadings of 0.1, 0.3, and 0.5 wt% Pd. Zirconium propoxide (Aldrich) and sulfuric acid precursors were then added to the solution to achieve final concentrations of 2.0 and 0.5 M, respectively. After 5 min of stirring, acetic acid was added as the hydrolyzing agent in an acid/zirconia ratio of 4:1. This solution was gently stirred, with gel formation occurring over approximately 3 h.

Upon gel formation the sample was transferred to a drying oven and dried overnight at 100 °C. After drying, the resulting powder was lightly ground using a mortar and pestle, and portions of the sample were calcined in air for 4 h at 500, 600, and 700 °C.

A sample of unloaded sulfated zirconia was also prepared. This material was prepared by the same method, lacking only the addition of Pd acetate to the sol.

2.2. BET surface area measurements

Measurements of catalyst surface areas and pore diameters were taken using nitrogen physisorption on a Micromeretics ASAP 2010. Before measurement, samples were pretreated overnight at a temperature of 130 °C and under a vacuum of 3 μmHg.

2.3. Catalytic activity testing

Catalyst activity measurements were taken for 0.1%, 0.3%, and 0.5%Pd/SZ samples calcined at 600 and 700 °C. Reactions were performed on an equal surface area basis. A catalyst sample of 12.5 m^2 surface area was loaded into a 1/4 in. o.d. stainless steel reactor tube and held in place between two plugs of quartz wool. Reaction temperatures were measured using a K-type thermocouple connected to an Omega 76000 temperature controller. Reactant concentrations were set using a series of Brooks 5850E mass flow controllers, in conjunction with a Brooks 0154 electronic control box. Reactant gas species were purchased from Praxair. Conditions used for the steady-state reaction studies were 1000 ppm NO_2, 3000 ppm CH_4, and 10% O_2 in balance He. Total gas flow was 45 cm^3/min.

Before beginning each steady-state reaction experiment, the catalyst samples were pretreated in 10% O_2/He for 30 min at 400 °C. Reaction measurements were taken in 50 °C increments from 300 to 600 °C. A Varian CP4900 MicroGC, equipped with molecular sieve 5A and PoraPLOT columns, was used for the quantification of O_2, N_2, N_2O, CH_4, CO, and CO_2. Neither N_2O nor CO were observed as products. NO and NO_2 were monitored using a Thermo Environmental Model 42H chemiluminescence NOx detector. Reported results were taken upon the reaction reaching steady-state, generally after 1–2 h on stream.

2.4. Thermogravimetric analysis/differential scanning calorimetry

Simultaneous thermogravimetric/differential scanning calorimetry measurements were performed on a Setaram TGA/DSC-111. Twenty-five milligrams of uncalcined sample was loaded

for each experiment. A flow of 5% O_2/He at 25 cm^3/min was introduced, and the sample held at 30 °C for 20 min to achieve a stable mass signal. A temperature ramp from 30 to 700 °C, at a rate of 5 °C/min was then begun.

2.5. Catalyst calcination monitored by mass spectrometry

The temperature-programmed calcination of sol–gel prepared catalysts was monitored by a Finnigan Trace DSQ mass spectrometer to examine evolved species during treatment. For these experiments, 100 mg of uncalcined catalyst sample was loaded into a quartz U-tube reactor. The sample was held in place between two plugs of quartz wool. Five percent O_2/He was introduced, at a flow rate of 30 cm^3/min, and the sample was flushed at room temperature for 15 min. After flushing, the sample temperature was raised from 25 to 700 °C at a ramp rate of 5 °C/min. Temperature was controlled using an Omega CSC32 controller.

2.6. In situ X-ray diffraction

The development of support crystallinity was monitored using *in situ* XRD. Experiments were performed using a Bruker D8 Advance diffractometer, which allows for controlled atmosphere and temperature, from cryogenic to 1200 °C. Samples precalcined at 500 °C were placed in a HTK 1200 controlled-atmosphere/controlled-temperature sample holder. Under a flow of 10 cm^3/min air, diffraction patterns were obtained at 25 °C steps between 500 and 700 °C. Samples were held at each temperature for 10 min before beginning the scans.

2.7. Laser Raman spectroscopy

Raman spectra of powdered catalyst samples were collected at room temperature using a Horiba Jobin-Yvon LabRam HR800 spectrometer. The laser source used was a Coherent Innova I70C-5 argon laser operating at a wavelength of 514.5 nm. Laser power at the samples was measured to be 2.0 mW. Reference samples of monoclinic and tetragonal zirconia were obtained from Saint-Gobain NorPro.

2.8. Diffuse reflectance IR spectroscopy

Infrared spectra were taken of 0.5%Pd/SZ samples which had been calcined at 500, 600, and 700 °C. Spectra were recorded on a Thermo Nicolet 6700 spectrometer. Catalysts samples were mixed to 10 wt% in KBr. Samples were loaded into an environmental chamber and treated at 200 °C in He for 30 min to remove adsorbed water. To examine the change in the catalyst surface between calcination temperatures, the spectrum of the sample calcined at 500 °C was used as the background for the other two samples.

NO adsorption was performed on the 0.5%Pd/SZ sample calcined at 600 °C as well as the corresponding palladium-free SZ support. The samples were pretreated in 20% O_2 at 400 °C for 30 min and then flushed with He, cooled to 50 °C, and background spectra were obtained. Adsorption was performed in 1000 ppm NO in He for 30 min at 50 °C, followed a 30 min. He flush, at which point the sample spectra were obtained and referenced to the corresponding background files.

3. Results and discussion

3.1. BET surface area

BET surface areas of the prepared catalysts are shown in Table 1. The addition of Pd to the sol–gel prepared SZ results in an increase in both the surface area and pore volume of the catalysts at a given calcination temperature. No trend was observed between surface area and Pd content of the catalysts. Additionally, both properties reach a maximum for each catalyst when it was calcined at 600 °C.

3.2. Steady-state reaction results

Fig. 1(a) shows the N_2 yields obtained during the reduction of NO_2 with CH_4 over 0.1, 0.3, and 0.5%Pd/SZ catalysts calcined at 600 °C. The observed N_2 yields are relatively low. N_2 yields over all three samples increased with reaction temperature up to a maximum, and then were seen to decrease. This trend is typical of the hydrocarbon reduction of NOx under lean conditions, and is due to the depletion of the reducing agent due to combustion at high temperatures. In the temperature range of 450–500 °C, the 0.3%Pd/SZ and 0.5%Pd/SZ catalysts reached N_2 yields of 32% and 24%, respectively. Below 450 °C, the 0.1%Pd/SZ catalyst showed lower activity, but N_2 yield increased with reaction temperature, reaching a maximum of 45% at 550 °C. N_2 yield was then observed to fall at 600 °C. The corresponding CH_4 conversions are shown in Fig. 1(b). CH_4 conversion over the 0.3%Pd/SZ and 0.5%Pd/SZ catalysts were very similar across

Table 1
Surface areas and pore volumes for catalysts prepared with different Pd loadings and at different calcination temperatures

Catalyst	Calcination temperature					
	500 °C		600 °C		700 °C	
	SA (m^2/g)	PV (cm^3/g)	SA (m^2/g)	PV (cm^3/g)	SA (m^2/g)	PV (cm^3/g)
0.5%Pd/SZ	55.4	0.20	100.6	0.27	68.5	0.23
0.3%Pd/SZ	45.9	0.18	101.9	0.21	64.7	0.19
0.1%Pd/SZ	66.4	0.23	103.2	0.27	80.2	0.25
SZ	44.3	0.18	85.6	0.22	61.8	0.22

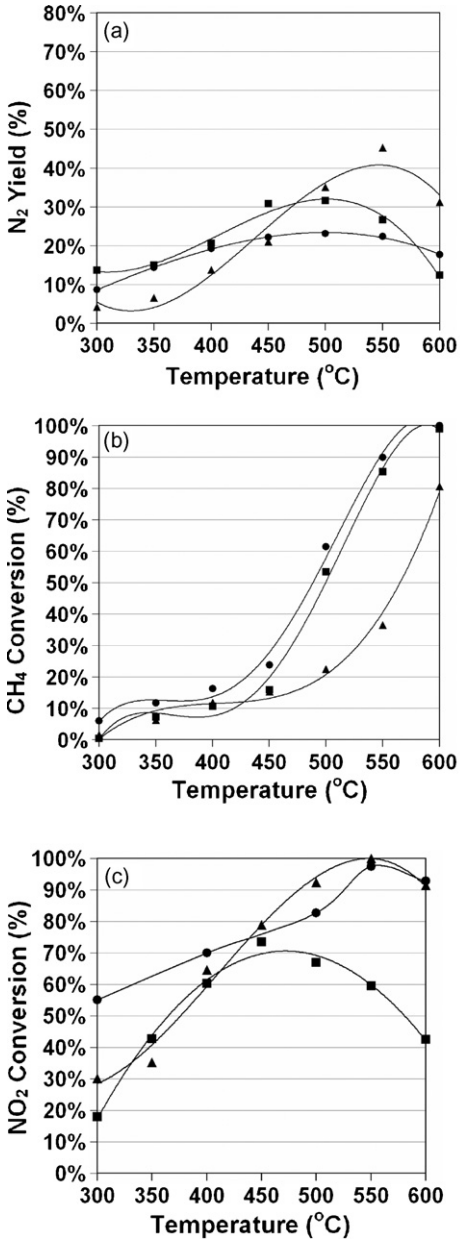

Fig. 1. (a) N_2 yield, (b) CH_4 conversion, and (c) NO_2 conversion during the reduction of NO_2 with CH_4 over (▲) 0.1%Pd/SZ, (■) 0.3%Pd/SZ, and (●) 0.5%Pd/SZ calcined at 600 °C.

the examined temperature range, although conversion of the 0.3%Pd/SZ sample was generally 5–10% lower at a given reaction temperature. CH_4 conversion took off sharply above 450 °C, corresponding to the maximum in N_2 yield over these catalysts. At 600 °C, complete conversion of CH_4 was observed for both the 0.3% and 0.5%Pd/SZ catalysts. The CH_4 conversions over 0.1%Pd/SZ were similar to the higher Pd-loaded samples at low temperatures, but deviated above 450 °C. The lower CH_4 conversion at high reaction temperatures could explain the observed shift and higher maxima observed in the N_2 yields over the 0.1%Pd/SZ sample.

The activity of the palladium-free support was also tested and it showed low N_2 yields (<10%) across the entire temperature range, and the CH_4 conversion was also much lower than for the Pd-containing samples (data not shown). The difference was especially pronounced at 450 °C and above, with Pd-free support showing less than half of the conversion levels seen over the Pd/SZ catalyst.

Fig. 1(c) shows the NO_2 conversion for the same set of experiments. At high temperatures, a decrease in the NO_2 conversions was observed, which follows a similar trend to the decline in the N_2 yield at higher temperatures. Analysis of N-containing products showed that N_2O was not produced and that conversion of NO_2 that did not result in N_2 formation was due to the partial reduction of NO_2 to form NO.

The samples that were calcined at 700 °C were also tested and the results are shown in Fig. 2. Significantly higher N_2 yields, shown in Fig. 2(a), were observed at each of the three Pd loadings when the catalysts were calcined at 700 °C, as opposed to 600 °C. Again, all three Pd-containing catalysts reached a maximum N_2 yield and showed the characteristic decrease at higher temperatures. Similar N_2 yields were observed on the 0.3%Pd/SZ and 0.5%Pd/SZ catalysts. The maximum N_2 yields on these samples were 65% and 69%, respectively, and were obtained at 450 °C. The increase in Pd loading from 0.3% to 0.5% seems to have resulted in an activity shift to slightly lower temperatures. Although these two catalysts had similar activity curves, N_2 yields below 450 °C were higher on the 0.5%Pd/SZ sample, while they were lower above this temperature. The activity shift to lower temperatures with increased metal loading is even more noticeable when these results are compared to the activity measurements on the 0.1%Pd/SZ catalyst. Over the 0.1%Pd/SZ sample, N_2 yield was observed to increase with temperature, reaching 66% at 500 °C. In fact, across the tested temperature range, a shift in activity of 50–100 °C higher temperatures was observed.

CH_4 conversions shown in Fig. 2(b) display a similar trend. CH_4 conversion at a given reaction temperature generally decreases with a decrease of Pd loading. This difference is small when comparing the 0.3%Pd/SZ and 0.5%Pd/SZ samples, as the methane conversions are similar, and both reach 100% at 550 °C. In comparison, CH_4 conversion is again shifted to higher temperatures on the 0.1%Pd/SZ sample, by about 50 °C.

The unloaded support was also tested and the N_2 yield was significantly lower (maximum yield <10%) than for the Pd-containing samples. The unloaded support calcined at 700 °C showed significantly lower methane conversion than the Pd-containing samples, reaching only 58% conversion at 600 °C.

The results displayed in Fig. 2(c) show that the NO_2 conversion profiles exhibit similar behavior to the N_2 yield profiles, going through a maximum as temperature is increased. These results indicate that higher Pd-loadings shift both NO_2 conversion and maximum N_2 yields to lower temperatures on these samples.

Comparison of CH_4 conversion between catalysts of the same Pd loading, but calcined at different temperatures, also reveals a trend. Methane conversions over the three Pd-containing

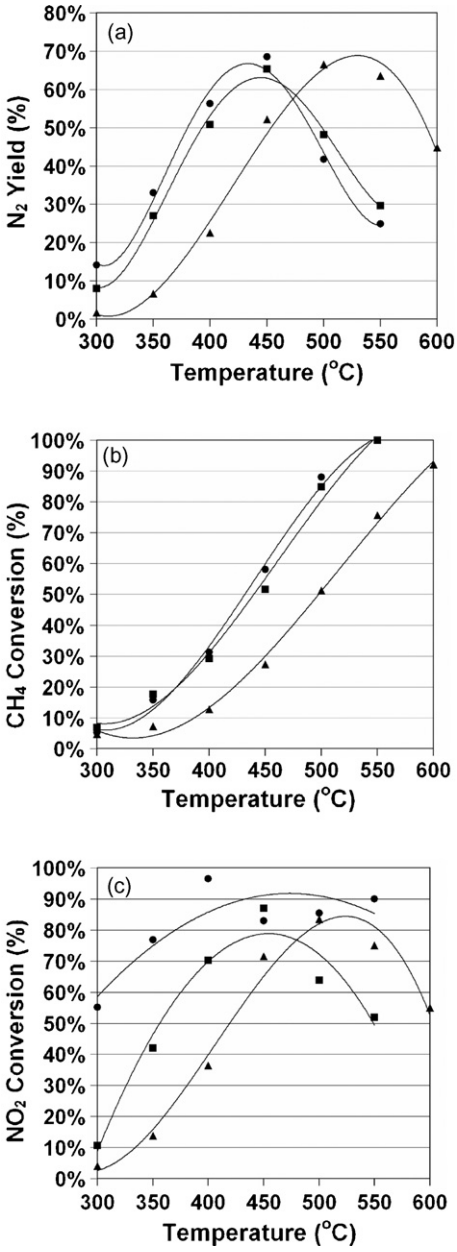

Fig. 2. (a) N_2 yield, (b) CH_4 conversion, and (c) NO_2 conversion during the reduction of NO_2 with CH_4 over (▲) 0.1%Pd/SZ, (■) 0.3%Pd/SZ, and (●) 0.5%Pd/SZ calcined at 700 °C.

catalysts calcined at 700 °C are shifted to lower reaction temperatures than observed over the samples calcined at 600 °C. Clearly, both Pd content and calcination temperature play a role in the activity of the catalysts for both the NO_2 reduction reaction and the combustion of CH_4 at high temperatures. Calcination at 700 °C significantly improves reduction activity and results in a lowering of the temperature at which maximum methane conversion is reached. When calcined at 700 °C, changes in the Pd loading did not result in significantly different N_2 yields. However, with increased Pd content, the maximum N_2 yields are reached at lower reaction temperatures. This effect is significant when increasing loading from 0.1% to 0.3%Pd, but less so with further Pd addition.

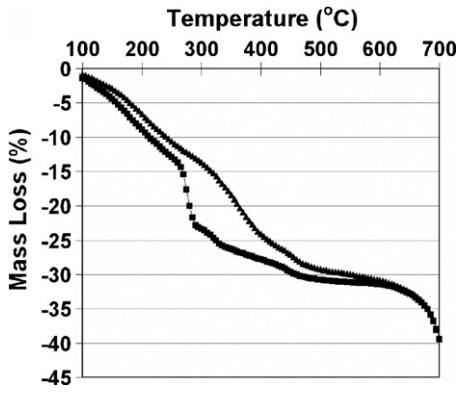

Fig. 3. Thermogravimetric measurement of the calcination of (▲) SZ and (■) 0.5%Pd/SZ.

3.3. 3.3 Thermogravimetric/differential scanning calorimetry and mass spectrometry

The calcination processes of the Pd-containing samples, as well as unloaded SZ, were examined using both TGA/DSC and mass spectrometry. With the combination of these techniques specific mass losses can be attributed to the evolution of gas species from the catalyst sample. Samples were pretreated under the same conditions in each set of experiments. The calcinations were performed in 5% O_2/He, and the samples were ramped from 30 to 700 °C at a rate of 5 °C/min. The TGA signals taken during the calcination of SZ and 0.5%Pd/SZ are shown in Fig. 3. Between 100 and 550 °C, the percentage mass loss is larger for the 0.5%Pd/SZ sample. The largest observed difference occurs at 265 °C, where a sharp mass loss of 10% was observed. Above 600 °C, the curves meet and overlap, indicating identical mass losses of 39% at 700 °C. The region of overlap included a high temperature mass loss of approximately 7%, which began around 650 °C. This large observed mass loss is typical of sol–gel preparations due to the removal of organic precursors at elevated temperatures.

To more effectively compare the TGA/DSC and MS data, the differential TGA signals (dTG) are presented in Fig. 4. Fig. 4(a) shows both the dTG and DSC data from the calcination of the unloaded SZ catalyst. Fig. 4(b) shows the MS calcination data for the same catalyst. During the calcination of sol–gel prepared SZ, dTG features were observed at 118, 190, 372, and 460 °C. A sharp mass loss is also observed starting at 650 °C. The two lowest dTG features correspond to a broad endothermic signal in the DSC data, and the removal of H_2O ($m/z = 18.17$) from the catalyst. H_2O evolution stops by 300 °C, and a broad CO_2 ($m/z = 44.28$) peak is observed then between 300 and 550 °C. This peak is centered at 380 °C, with a shoulder at 460 °C. An exothermic peak at 380 °C coincides with the production of CO_2. The loss of sulfur from the catalysts is observed through the ions of SO_2 ($m/z = 64.48$). The evolution of SO_2 was first observed above 350 °C, and increased slowly with temperature until a sharp peak at 645 °C. The corresponding DSC and dTG show an endothermic mass loss.

Data from the calcination of 0.1%Pd/SZ are shown in Fig. 5(a) and (b). As in the calcination of the unloaded SZ, dTG

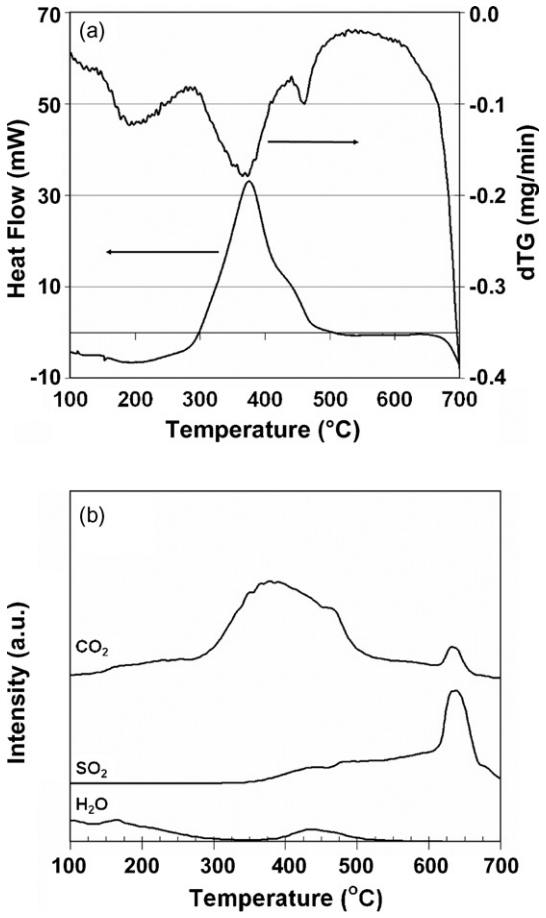

Fig. 4. (a) DSC and dTG profiles and (b) corresponding MS signals for CO_2, SO_2, and H_2O collected during the calcination of sol–gel prepared SZ.

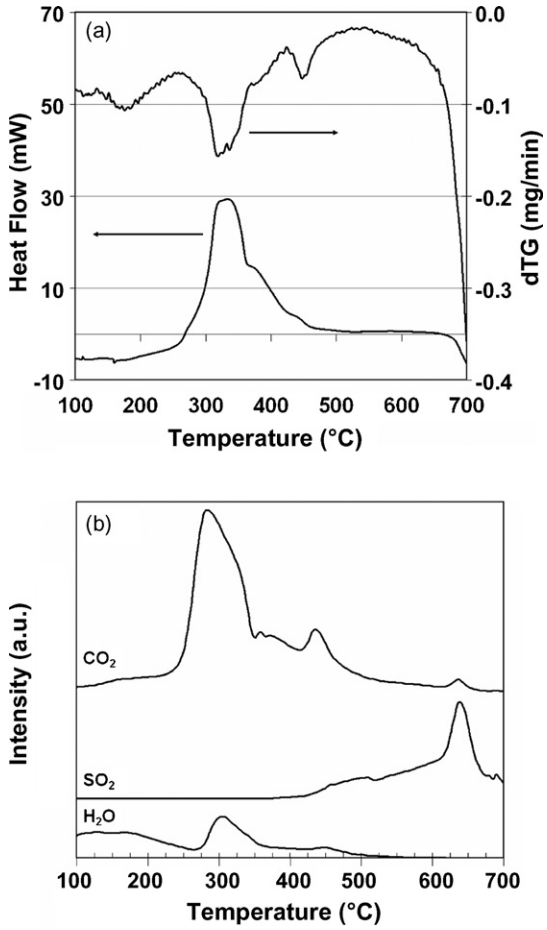

Fig. 5. (a) DSC and dTG profiles and (b) corresponding MS signals for CO_2, SO_2, and H_2O collected during the calcination of sol–gel prepared 0.1%Pd/SZ.

peaks at 117 and 175 °C correspond to the desorption of H_2O from the catalyst. Additionally, an endothermic peak and mass loss occur with loss of SO_2 above 650 °C. Although the main peak in the MS SO_2 signal occurs at the same temperature as in SZ, it was noted that sulfur loss did not start until above 400 °C, showing a shift to slightly higher temperature. The main difference was in the evolution of CO_2 from the sample. The intensity and shape of both the dTG and DSC peaks were close to those seen for SZ, however, a shift to lower temperature was observed. The DSC peak began around 250 °C and was centered at 330 °C, with a shoulder at 380 °C. In the MS, the CO_2 was observed as a sharp peak at 300 °C and shoulder at 375 °C. A second small peak was also seen at 440 °C.

Fig. 6(a) and (b) show the dTG/DSC and MS data taken during the calcination of 0.3%Pd/SZ. The desorption of H_2O was again observed below 250 °C in all three signals. A sharp SO_2 desorption peak was observed at 645 °C, however the gradual loss of SO_2 at temperatures below this was less intense than for the SZ and 0.1%Pd/SZ catalysts. Additionally, the evolution of CO_2 from the catalyst samples occurred over a significantly narrowed temperature range. The observed exothermic feature occurs between 250 and 350 °C. Along with narrowing, the heat flow reached 46.5 mW. Two distinct DSC peaks were observed at 270 and 315 °C, which were matched in both the dTG and CO_2 signals. As with the DSC, these peaks both narrowed and increased in intensity.

With the further increase in Pd content to 0.5%, the trends noted for the previous samples were observed to continue. Fig. 7(a) and (b) contain the data on the calcination of 0.5%Pd/SZ. As with the 0.3%Pd/SZ sample, the desorption of SO_2 began near 450 °C and was relatively low below 600 °C. The main SO_2 desorption peak again occurs near 650 °C, but was broadened in comparison to the other catalyst samples. A distinct shoulder was seen at 680 °C. The evolution of CO_2 from the sample was again shifted to lower temperature with the MS peak centered at 280 °C. Both the DSC and dTG signals showed corresponding peaks, which were narrowed and of greater intensity than in the 0.3%Pd/SZ sample. The exothermic DSC peak reached a maximum heat flow of 135 mW while the dTG reached −0.7 mg/min. A smaller second peak at 325 °C was visible in the DSC and dTG data but was not resolved in the MS signal. The MS did show a second small peak at 450 °C, as was observed in the other samples.

With the addition of increasing amounts of Pd to the sol–gel SZ catalyst, the evolution of CO_2 during calcination occurs at much lower temperatures. As evidenced by the narrowed and more intense DSC peaks, the rate of CO_2 evolution is also seen to increase. CO_2 produced during calcination is due to the com-

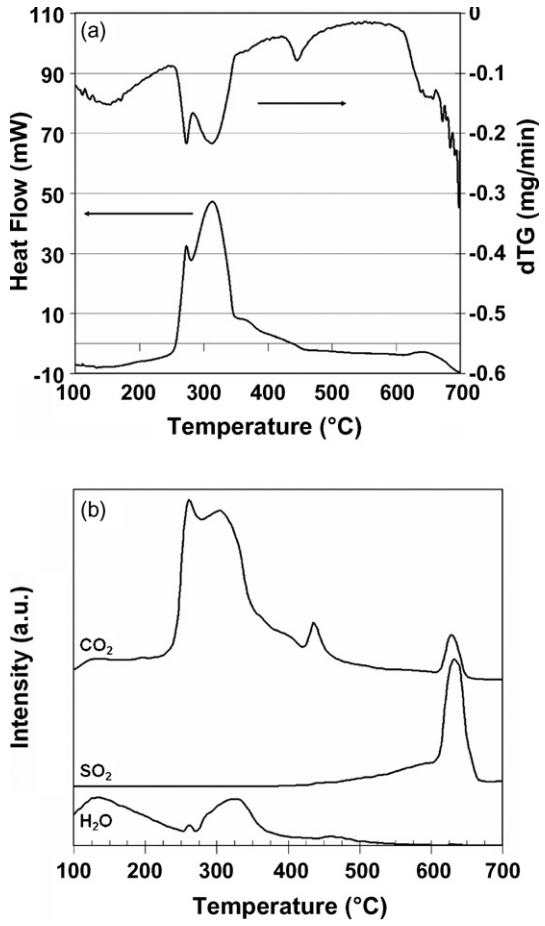

Fig. 6. (a) DSC and dTG profiles and (b) corresponding MS signals for CO_2, SO_2, and H_2O collected during the calcination of sol–gel prepared 0.3%Pd/SZ.

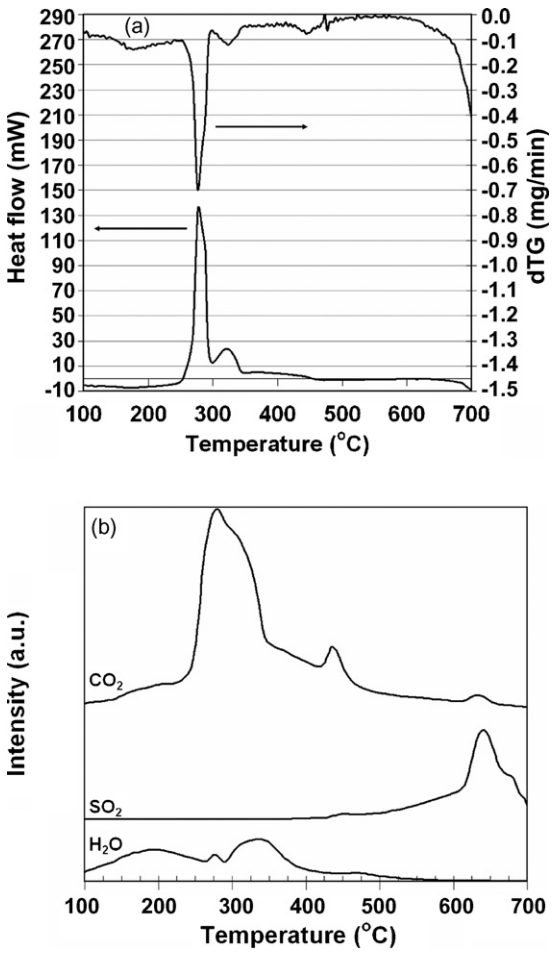

Fig. 7. (a) DSC and dTG profiles and (b) corresponding MS signals for CO_2, SO_2, and H_2O collected during the calcination of sol–gel prepared 0.5%Pd/SZ.

bustion of the organic sol–gel precursors. It is likely, therefore, that the observed change is due to Pd catalyzing the combustion reaction. With increased Pd content, the loss of SO_2 during calcination is somewhat reduced below 600 °C. It does not, however, seem to have much of an effect at higher temperatures, as the main loss of sulfur occurs near 650 °C for all four catalysts tested.

3.4. In situ X-ray diffraction

The effect of Pd-content on the formation of zirconia crystallites was examined through *in situ* calcination by XRD. Diffraction patterns were taken in 25 °C steps between 500 and 700 °C. Samples were held at each temperature for 10 min before scans were begun. The diffraction patterns during the calcination of 0.5%Pd/SZ, which were similar to those obtained on the other samples, are shown in Fig. 8. All four catalyst samples (0.0, 0.1, 0.3, and 0.5%Pd/SZ) showed the presence of only the tetragonal zirconia phase, as evidenced by the [1 1 1] ($2\theta = 30.2°$), [2 0 2] ($2\theta = 50.2°$), and [1 3 1] ($2\theta = 60.2°$) diffraction lines. In the unloaded SZ sample, diffraction lines were first observed at 600 °C and sharpened with increasing calcination temperature. Formation of the monoclinic zirconia phase, which could be identified by the [−1 1 1], [1 1 1], and [−1 1 2] diffraction lines at respective 2θ values of 28.5°, 31.5°, and 40.7°, where not observed. This is consistent with other one-step sol–gel preparations in the literature [11,13]. With the addition of 0.1%Pd very low intensity peaks were observed beginning at 575 °C. With further increases in Pd loading (0.3% and 0.5%), stronger tetragonal

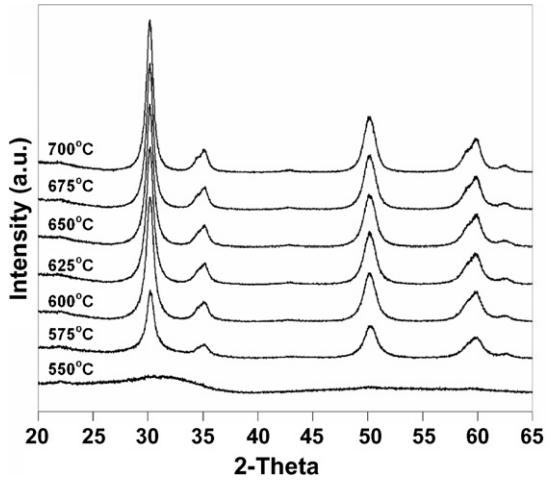

Fig. 8. XRD patterns taken during the calcination of sol–gel prepared 0.5%Pd/SZ.

Table 2
Zirconia crystallite sizes observed during *in situ* calcination

Catalyst	Calcination temperature					
	575 °C	600 °C	625 °C	650 °C	675 °C	700 °C
SZ	–	13.3	13.7	13.9	14.4	14.7
0.1%Pd/SZ	–	13.9	14.2	14.4	15.5	16.1
0.3%Pd/SZ	13.5	15.8	15.5	16.1	16.5	17.9
0.5%Pd/SZ	14.7	16.8	17.5	17.5	18.7	18.7

Effect of temperature and Pd loading.

zirconia peaks formed at 575 °C. The highest peak intensities were seen in the 0.5%Pd/SZ sample. These results indicate that the addition of Pd prior to the gelation step results in the formation of zirconia crystallites at lower temperatures. Calculation of crystallite size using the Scherrer equation demonstrated that increased Pd loading also resulted in increased zirconia crystallite size at a given calcination temperature. These complete results are presented in Table 2. Observed crystallite sizes were in the range of 13–19 nm.

3.5. Raman spectroscopy

Raman spectra of the sol–gel prepared 0.5%Pd/SZ samples were taken after calcination at 500, 600, and 700 °C. These results are shown in Fig. 9, along with reference samples of the monoclinic and tetragonal zirconia phases. The 0.5%Pd/SZ calcined at 500 °C displayed no Raman bands, which can be attributed to the lack of crystallinity at this calcination temperature, which was also observed by XRD. For the sample calcined at 600 °C, characteristic bands of the tetragonal ZrO_2 phase were observed at 148, 273, 318, 468, and 648 cm^{-1}, which was consistent with our reference sample, the literature [28–36], and

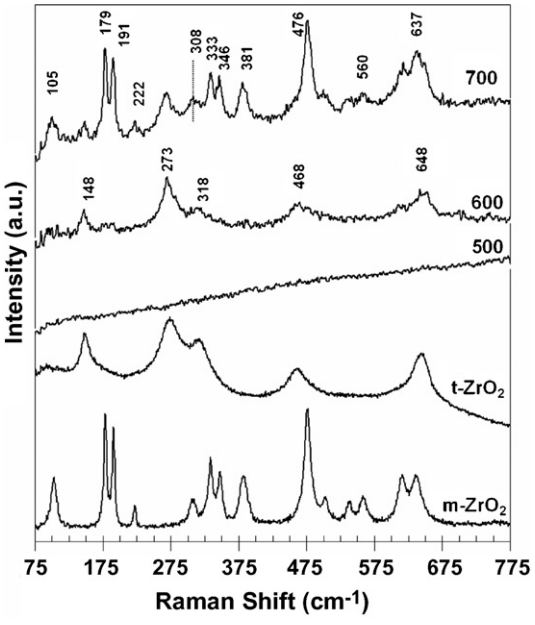

Fig. 9. Raman spectra of 0.5%Pd/SZ prepared by and calcined at different temperatures. Spectra of commercial monoclinic and tetragonal ZrO_2 materials also shown for reference.

our XRD results. The Raman spectra of the sample calcined at 700 °C contained all of the bands assigned to tetragonal ZrO_2, which were also observed in the sample calcined at 600 °C, but several new bands from monoclinic ZrO_2 were observed to appear. The most prominent features appeared at 105, 179, 191, 222, 333, 346, 381, 476, 560, and 637 cm^{-1} and closely matched the reference sample. Kim and Hamaguchi used an isotopic exchange technique to assign these ZrO_2 bands [36]. They assigned the bands at 333, 222, 191, and 179 cm^{-1} to Zr–Zr vibrations. Bands at 381, 346, and 308 were due to Zr–O vibrations. The Raman bands at 637, 560, 476, and 105 cm^{-1} were assigned to O–O vibrations.

The observation of both the tetragonal and monoclinic ZrO_2 phases in the 700 °C sample is in contrast with the *in situ* XRD results, which showed no evidence of the monoclinic phase at 700 °C. Li et al. [29,37] examined this phase transformation in several ZrO_2 samples, including sulfated zirconia. By comparing UV Raman, visible Raman, and XRD data, they proposed that the transition from the tetragonal to the monoclinic phase begins at the surface and proceeds into the bulk support. The results presented here are consistent with such a model, as the monoclinic phase was only observed through the more surface sensitive Raman spectroscopy and not in the bulk sampling XRD [29,37]. Additionally, the surface phase transformation was observed after the loss of sulfate species, observed at 650 °C in the mass spectrometry experiments. The presence of surface sulfate groups is known to stabilize the tetragonal ZrO_2 phase, and the loss of these species may prompt the transformation from tetragonal to monoclinic ZrO_2.

3.6. IR spectroscopy

DRIFTS was used to examine the changes in the catalyst surface as calcination temperature was changed. DRIFTS spectra of 0.5%Pd/SZ calcined at 500, 600, and 700 °C were obtained. Fig. 10(a) shows the spectrum obtained from the sample calcined at 500 °C. To highlight the changes in the spectra, the spectrum from the sample calcined at 500 °C was subtracted from the samples calcined at higher temperatures, which are shown in Fig. 10(b). On the sample calcined at 500 °C, a band at 1620 cm^{-1} assigned to the bending vibration of OH groups on the surface was detected. Also, a broad feature was observed in the sulfate region between 1000 and 1400 cm^{-1}. This broad band, which is centered around 1195 cm^{-1} is attributed to the SO_4^{2-} ion and symmetric stretching mode of O=S=O in $(Zr)_2SO_2$ [38,39]. Other bands were not well-resolved.

Comparing the sample calcined at 500 °C with the ones calcined at 600 and 700 °C, as shown by the difference spectra in Fig. 10(b), reveals several changes. For the sample calcined at 600 °C, the OH band was seen to decrease in intensity and to shift to a slightly lower wavenumber, which can be seen from the small negative band at 1620 cm^{-1} and small positive band at 1606 cm^{-1} in the difference spectra. Li and Gonzalez [40] observed similar behavior during dehydration of a sol–gel prepared SZ sample. The positive bands near 1386 and 1370 cm^{-1} are commonly attributed to the asymmetric $\nu_{S=O}$ stretch on

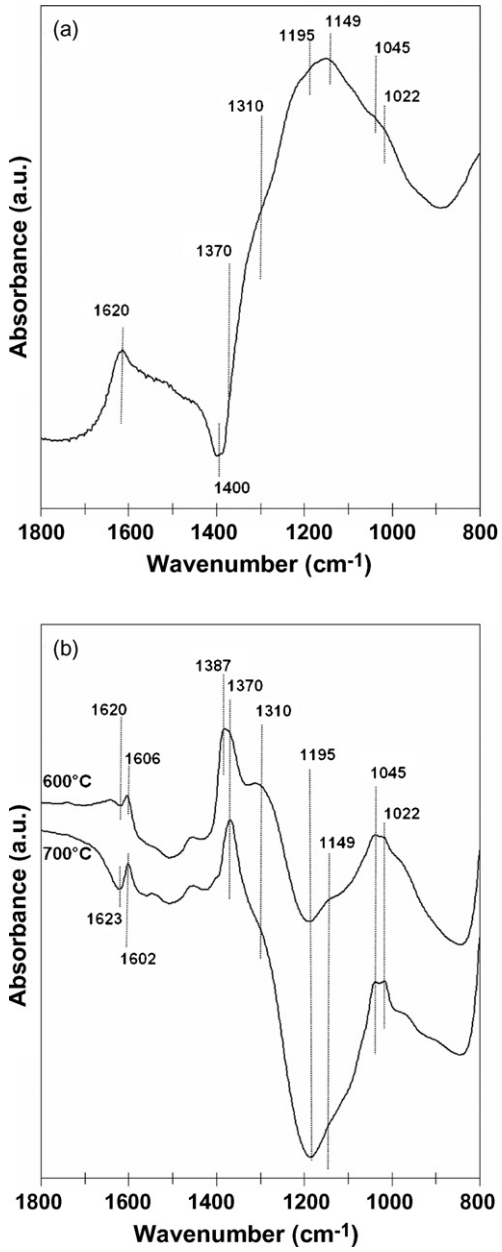

Fig. 10. DRIFTS spectra of 0.5%Pd/SZ calcined at (a) 500 °C, and (b) difference spectra of samples calcined at 600 and 700 °C (sample calcined at 500 °C used as background).

sulfated zirconia samples [39], either as the $\nu_{S=O}$ mode of surface $(ZrO)_3S{=}O$ species or the asymmetric O=S=O stretch of $(ZrO)_2SO_2$ [38]. The shoulder band at 1310 cm^{-1} on the sample calcined at 600 °C, that disappears for the sample calcined at 700 °C, has been attributed to the transformation of the bidenate SO_4^{2-} ion by dehydration, which is also accompanied by a decrease in absorbance at 1195 cm^{-1} [39]. A large overall decrease in absorbance in the sulfate region was observed, shown by the negative band at centered at 1195 cm^{-1} that becomes more negative with increased calcination temperature. This band has been attributed to the SO_4^{2-} ion [39] and symmetric stretch of O=S=O in $(Zr)_2SO_2$ species [38,41]. Such a decrease is expected, based upon the previously discussed MS data, due to SO_2 desorption. The shoulder band at 1149 cm^{-1}, that is present in the difference spectra for the sample calcined at 600 °C but disappears in the 700 °C difference spectra, is due to the symmetric O=S=O stretch in bidentate sulfates [41,42].

Bands at 1045 and 1022 cm^{-1} were also observed. These bands arise from the ν_{S-O} stretching mode(s) of all surface sulfates [38,43] and are typical of more highly dehydrated species, which can be explained by greater dehydration of the samples calcined at 600 and 700 °C as compared to the one calcined at 500 °C [38,39,42,43]. The OH band in the 0.5%Pd/SZ catalyst calcined at 700 °C showed a further decrease in intensity and shift to lower wavenumbers, indicated by the negative band at 1623 cm^{-1} and positive band at 1602 cm^{-1}.

Consideration of the DRIFTS data and previously discussed characterization studies may be used to shed light on the observed NO_2 reduction reaction results. Crystallinity was not observed in the sample calcined at 500 °C. This corresponded to a lack of IR bands showing sulfates attached to the zirconia support. Calcination at 600 °C results in the formation of both the tetragonal zirconia phase, as well as the development of bidentate sulfate species which are coordinated with zirconia. While these samples were active for the reduction of NO_2 with CH_4, they were significantly less active than catalysts calcined at 700 °C. Although a significant loss of sulfates occurred near 650 °C during sample calcination, sulfate species clearly remained on the catalyst surface, and the formation of S=O species was observed in the sample treated at 700 °C. This improvement in activity is similar to results observed by both Ward and Ko [13,44] and Armendariz et al. [16]. The latter group demonstrated higher activities for the hydroconversion of n-hexane on sulfated zirconia samples treated at temperatures above 600 °C, corresponding to monolayer sulfate coverage. Here, we have shown a similar trend in activity for the reduction of NO_2 with CH_4, with sol–gel SZ catalysts calcined at 700 °C being capable of high N_2 yields.

The remaining question, with regard to catalytic activity for NO_2 reduction, is the state of Pd in the various catalysts. Due to low concentration and overlap of characteristic XPS peaks, determining the surface state of Pd in sulfated zirconia is difficult. Resasco [7] had made use of EXAFS to show that the state of Pd in the active reduction catalyst is dispersed Pd^{2+} ions. In comparison, PdO is highly selective for the combustion of CH_4. Activity of these catalysts for the selective reduction reaction would therefore argue for the presence of dispersed Pd species in these sol–gel samples. Shifts in activity to lower temperatures with an increase in Pd content may simply be due to a resulting increase in Pd on the surface. We have previously observed such a shift on samples prepared by incipient wetness techniques [25].

Fig. 11 shows the DRIFTS spectra at 50 °C after NO adsorption and flushing for the 0.5%Pd/SZ and unloaded SZ catalysts calcined at 600 °C. The incorporation of Pd led to some differences in the NO adsorption spectra. The negative bands at 3753 and 3651 cm^{-1} are attributed to NO interaction with surface hydroxyl groups [45,46]. Hadjiivanov et al. have reviewed FT-IR assignments of adsorbed NOx species and also examined NO adsorption on ZrO_2 and sulfated ZrO_2 [47,48]. The

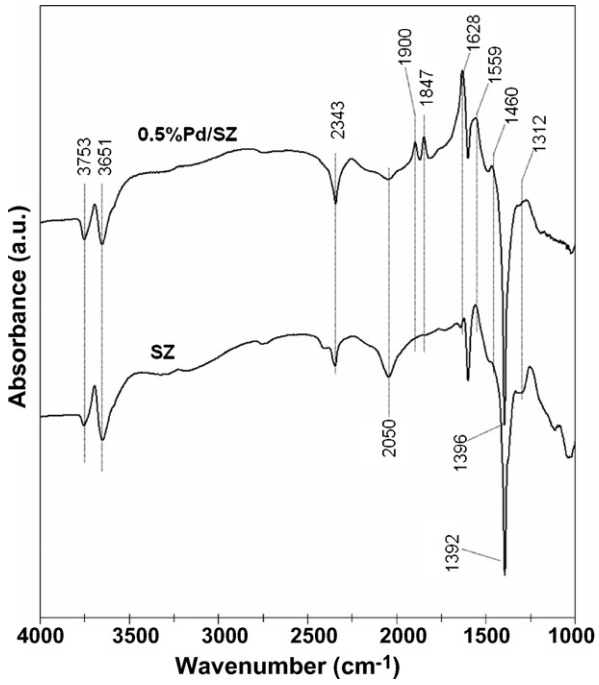

Fig. 11. DRIFTS spectra at 50 °C after NO adsorption on 0.5%Pd/SZ and Pd-free SZ calcined at 600 °C.

band at 2343 cm^{-1} may be attributed to residual carbonates that produced CO_2 during activation of the sample, which was then removed through the flushing and adsorption steps. This feature is less prominent in the Pd/SZ sample than the unloaded SZ support, which is consistent with TGA/DSC/mass spectrometry results during the calcination, which showed the organic precursors decomposed at lower temperatures to form CO_2 in the Pd-containing samples than on the Pd-free SZ support. The negative band at 2050 cm^{-1} is due to NO interaction with the first overtones of the ν(S-O) mode [49]. The bands at 1900 and 1847 cm^{-1} are due to NO interaction with Pd species stabilized by the support, as they are absent in the Pd-free sample. Studies on NO adsorption on Pd catalysts in similar systems [50–52] have been carried out and the bands at 1900 and 1847 cm^{-1} may be attributed to NO adsorbed on Pd^{2+} cations in different environments. It has been proposed that on sulfated zirconia, protons associated with SO_4 groups serve to stabilize Pd^{2+} [51]. The absence of any significant absorbance bands around 1740 and 1660 cm^{-1} indicates little or no adsorption of NO on metallic Pd [52]. The band at 1900 cm^{-1} has also been attributed to the ν(N–O) stretch of linearly adsorbed NO on $Zr^{4+}(SO_4{}^{2-})$ or in N_2O_3 species [47], but the absence of this band from the unloaded SZ helps support the assignment to NO adsorbed on Pd cations. The asymmetric stretch from bridging nitrates at 1628 cm^{-1} and bidentate nitrates at 1559 cm^{-1} was also detected. The asymmetric ν_{as}(N–O) mode of monodentate nitrates gives rise to the absorbance at 1460 cm^{-1}. The sharp negative band near 1400 cm^{-1}, due to the asymmetric O=S=O stretching mode, shows a strong interaction of the sulfate groups with NO [12,21,47]. The band at 1312 cm^{-1} has been credited to the asymmetric stretch of nitro species or monodentate nitrates.

4. Conclusions

The preparation of Pd/SZ catalysts through a single step sol–gel technique has been shown to result in catalysts active for the reduction of NO_2 with CH_4 under lean conditions. The addition of increasing amounts of Pd to the catalyst resulted in a lowering of the temperature window of maximum N_2 yield. Addition of Pd to the sol–gel preparation also resulted in the evolution of organic precursors and the formation of the crystalline support at lower calcination temperatures.

Reaction results over sol–gel Pd/SZ catalysts calcined at 600 and 700 °C showed that the higher calcination temperature resulted in more active catalysts for the reduction of NO_2 with CH_4. Characterization of the catalysts has shown several key differences in these samples. Although XRD indicates that the bulk support consisted of only the tetragonal ZrO_2 phase in both samples, Raman spectroscopy indicates a change in the surface phase to monoclinic ZrO_2. This transition seems to correspond to a loss of sulfate species near 650 °C during catalyst calcination. In addition to the observed surface phase change, calcination at 700 °C also resulted in changes to surface sulfate species as observed by IR spectroscopy, and the formation of stable bidentate sulfate groups. At 600 °C, evidence of sulfate coordination to Zr atoms is observed. In the 700 °C samples, although a general decrease in intensity was observed, these bonds remained intact, and an additional band corresponding to S=O stretching was observed. The ZrO_2 phase transition is commonly observed to correspond to a decrease in reaction activity. This is not the observed case for these samples; however, there may be competing effects of calcination temperature. We have previously shown that by performing the easier reduction of NO_2 (as compared to NO), high N_2 yields can be attained using Pd on sulfated monoclinic zirconia, prepared by incipient wetness impregnation [25]. Thus, the phase transition from tetragonal to monoclinic zirconia may be less important in this application. Alternatively, the achievement of monolayer sulfate coverage and the full formation of surface acid sites may explain the activity improvement.

Acknowledgements

We gratefully acknowledge the funding provided for this work by the United States Department of Energy (DOE) and the National Energy Technology Laboratory (NETL) through the cooperative agreement DE-FC26-02NT41610.

References

[1] M. Iwamoto, H. Hamada, Catal. Today 10 (1991) 57.
[2] M. Iwamoto, H. Yahiro, Catal. Today 22 (1994) 5.
[3] Y. Nishizaka, M. Misono, Chem Lett. (1993) 1295.
[4] Y. Nishizaka, M. Misono, Chem. Lett. (1994) 2237.
[5] C.J. Loughran, D.E. Resasco, Appl. Catal. B: Environ. 7 (1995) 113–126.
[6] Y.-H. Chin, W.E. Alvarez, D.E. Resasco, Catal. Today 62 (2000) 159–165.
[7] A. Ali, W. Alvarez, C.J. Loughran, D.E. Resasco, Appl. Catal. B: Environ. 14 (1997) 13–22.
[8] B.J. Adelman, W.M.H. Sachtler, Appl. Catal. B 14 (1997) 1.
[9] H. Ohtsuka, Appl. Catal. B 33 (2001) 325.

[10] H. Ohtsuka, T. Tabata, T. Hirano, Appl. Catal. B 28 (2000) L73.
[11] K. Arata, Adv. Catal. 37 (1990) 165.
[12] V. Parvulescu, S. Coman, V.I. Parvulescu, P. Grange, G. Poncelet, J. Catal. 180 (1998) 66.
[13] D.A. Ward, E.I. Ko, J. Catal. 150 (1994) 18.
[14] D. Tichit, B. Coq, H. Armendariz, F. Figueras, Catal. Lett. 38 (1996) 109.
[15] K. Biro, F. Figueras, C. Marquez Alvarez, S. Bekassy, J. Valyon, J. Therm. Anal. Cal. 56 (1999) 345–353.
[16] H. Armendariz, B. Coq, D. Tichit, R. Dutartre, F. Figueras, J. Catal. 173 (1998) 345–354.
[17] M.K. Mishra, B. Tyagi, R.V. Jasra, J. Mol. Catal. A: Chem. 223 (2004) 61–65.
[18] S. Ardizzone, C.L. Bianchi, G. Cappelletti, F. Porta, J. Catal. 227 (2004) 470.
[19] D.J. Rosenberg, F. Coloma, J.A. Anderson, J. Catal. 210 (2002) 218.
[20] T. Lopez, F. Tzompantzi, J. Navarrete, R. Gomez, J.L. Boldu, E. Munoz, O. Novaro, J. Catal. 181 (1999) 285.
[21] C. Morterra, G. Cerrato, S. Di Ciero, M. Signoretto, F. Pinna, G. Strukul, J. Catal. 165 (1997) 172.
[22] M.W. Kumthekar, U.S. Ozkan, J. Catal. 171 (1997) 45.
[23] J. Mitome, E. Aceves, U.S. Ozkan, Catal. Today 53 (1999) 597.
[24] G. Karakas, J. Mitome-Watson, U.S. Ozkan, Catal. Commun. 3 (2002) 199.
[25] E.M. Holmgreen, M.M. Yung, U.S. Ozkan, Catal. Lett. 111 (1-2) (2006) 19.
[26] E.M. Holmgreen, M.M. Yung, U.S. Ozkan, Appl. Catal. B, accepted for publication.
[27] L.B. Hamouda, A. Ghorbel, J. Sol–gel Sci. Technol. 19 (2000).
[28] T. Hirata, J. Phys. Chem. Solids 56 (1995) 951.
[29] M. Li, Z. Feng, G. Xiong, P. Ying, Q. Xin, C. Li, J. Phys. Chem. B 105 (2001) 8107.
[30] A.A. Sobol, Y.K. Voronko, J. Phys. Chem. Solids 65 (2004) 1103.
[31] P.E. Quintard, P. Barberis, A.P. Mirgorodsky, T. Merle-Mejean, J. Am. Ceram. Soc. 85 (2002) 1745.
[32] D.-J. Kim, H.-J. Jung, J. Am. Ceram. Soc. 76 (1993) 2106.
[33] D. Michel, L. Mazerolles, M. Perez y Jorba, J. Mater. Sci. 18 (1983) 2618.
[34] A.P. Mirgorodsky, M.B. Smirnov, P.E. Quintard, J. Phys. Chem. Solids 60 (1999) 985.
[35] P. Bouvier, G. Lucazeau, J. Phys. Chem. Solids 61 (2000) 569.
[36] B.-K. Kim, H.-O. Hamaguchi, Phys. Stat. Sol. (b) 203 (1997) 557.
[37] C. Li, M. Li, J. Raman Spectrosc. 33 (2002) 301.
[38] C. Morterra, G. Cerrato, F. Pinna, M. Signoretto, G. Strukul, J. Catal. 149 (1994) 181.
[39] F. Babou, G. Coudurier, J.C. Vedrine, J. Catal. 152 (1995) 341.
[40] B. Li, R.D. Gonzalez, Catal. Today 46 (1998) 55–67.
[41] J.R. Sohn, H.W. Kim, J. Mol. Catal. 52 (1989) 361.
[42] M.A. Ecormier, K. Wilson, A.F. Lee, J. Catal. (2003) 57.
[43] T. Yamaguchi, T. Jin, K. Tanabe, J. Phys. Chem. 90 (1986) 3148.
[44] D.A. Ward, E.I. Ko, J. Catal. 157 (1995) 321.
[45] J.M. Watson, U.S. Ozkan, J. Catal. 210 (2002) 295.
[46] J.M. Watson, U.S. Ozkan, J. Mol. Catal. A 192 (2003) 79.
[47] K. Hadjiivanov, V. Avreyska, D. Klissurski, T. Marinova, Langmuir 18 (2002) 1619.
[48] K.I. Hadjiivanov, Catal. Rev.—Sci. Eng. 42 (2000) 71.
[49] M. Kantcheva, A.S. Vakkasoglu, J. Catal. 223 (2004) 352.
[50] A.W. Aylor, L.J. Lobree, J.A. Reimer, A.T. Bell, J. Catal. 172 (1997) 453.
[51] Y.-H. Chin, A. Pisanu, L. Serventi, W.E. Alvarez, D.E. Resasco, Catal. Today 54 (1999) 419.
[52] C. Descorme, P. Gelin, M. Primet, C. Lecuyer, Catal. Lett. 41 (1996) 133.